# Characterization of speckle/despeckling in active millimeter wave imaging systems using a first order 1.5D model

I.Ocket[*], B. Nauwelaers[*], J. Fostier[#], L. Meert[#], F. Olyslager[#], G. Koers[°], J. Stiens[°], R. Vounckx[°], I. Jager[°]

[*] K.U.Leuven, ESAT/Telemic, Kasteelpark Arenberg 10, 3001 Heverlee Belgium;
[#] UGent, Division INTEC, St-Pietersnieuwstraat 41, 9000 Ghent, Belgium;
[°] Vrije Universiteit Brussel, Division ETRO, Pleinlaan 2, 1050 Elsene, Belgium

## ABSTRACT

In this paper a simplified "1.5D" modeling approach is presented which can be used to characterize and optimize an entire active millimeter wave imaging system for concealed weapon detection. The method uses Huygens' Principle to compute one field component on selected planes of the imaging set-up. The accuracy of the method is evaluated by comparing it to a rigorous 2D method of moments approach. The model includes the effects of lenses, diffusers, mirrors, object and any other component present in the system. The approach allows fast determination of the influence of each of the system components on the image projected onto the sensor, including effects such e.g. speckle. Also, the effectivity of different speckle reduction techniques, e.g. using a Hadamard diffuser or a multifrequency approach are evaluated in this paper.

**Keywords:** active millimeter wave imaging, Hadamard, speckle, method of moments, Huygens

## 1. INTRODUCTION

Active millimeter wave imaging systems [1-3]are considered one of the most promising systems for the development of all-round versatile indoor security applications. In an indoor environment an active imaging approach is needed to achieve a sufficient difference in radiation temperature between the objects to be imaged and the background noise level of a typical indoor environment. In active imaging the scene to be imaged is illuminated with a radiation source, comparable to a flashlight in optical imaging. However, an important difference is that at mm-wave frequencies truly incoherent sources are difficult to realize so the resulting problem of speckle will have to be dealt with. Speckle occurs when scattered radiation from objects or rough surfaces randomly destructively interferes and degrades image smoothness.

A generic system set-up is shown in Fig. 1 that uses a refectarray (diffuser) which can be switched between different phase patterns in order to destroy the coherence of the incident radiation. A sum over the different phase settings at the detector side can then reduce speckle in the averaged image.

When designing a complex system such as this, a fast way of estimating the influence of various system components (lenses, mirrors, diffuser, object, etc.) on system performance is a very useful tool. Since a full-wave 3D calculation on the system level is not practical we will use a simplified approach which is still able to model all the necessary system features. In [4], the authors mention that analytical treatment of these systems is only possible for the different components separately and that this approach doesn't yield an optimized performance on the system level. Thus some type of hybrid solution is suggested which combines Gaussian beam propagation, ray tracing and diffraction calculations. In this paper this is the approach taken, where the illumination of the object is treated with Gaussian beam theory while the rest of the system is treated using an approach based on Huygens' Principle.

Interesting parameters to investigate are frequency, lens diameters and focal distances, effects of object shape, effect of diffuser phase patterns, power requirements, etc. The speed of the calculation will also enable to quickly evaluate the effectivity of despeckling techniques such as the one suggested in Fig. 1, but also broadband imaging techniques.

In this paper, we will first give some background and motivation for our research. After this, in a first section, the proposed 1.5D method is described in detail. A second section will present the 2D method used as a reference to the 1.5D method. A simplified reference system set-up is then described in a third section and simulated with both methods.

Millimeter-Wave and Terahertz Photonics, edited by Dieter Jäger, Andreas Stöhr,
Proc. of SPIE Vol. 6194, 619409, (2006) · 0277-786X/06/$15 · doi: 10.1117/12.661689

To further illustrate the method and study the effect of lens characteristics a set of simulations is presented in a fourth section for the combination of object, detector lens and detector.

The subsequent sections deal with the characterization of speckle and despeckling techniques. A fifth section presents a simple way of modeling rough surfaces on the object, which is then used in the sixth section to study the effectiveness of two despeckling techniques: the first one uses a Hadamard diffuser to destroy the coherence of the illuminating technique while in the second approach multiple frequencies are used to achieve despeckling. In these two sections a start is made in the modeling and description of these despeckling techniques using the 1.5D method. In a final section we will reach some first, tentative conclusions.

This work was partially funded by the Vrije Universiteit Brussel (VUB-OZR), the Flemish Fund for Scientific Research (FWO- G.0041.04) and the Flemish Institute for the encouragement of innovation in science and technology (IWT-SBO 231.011114).

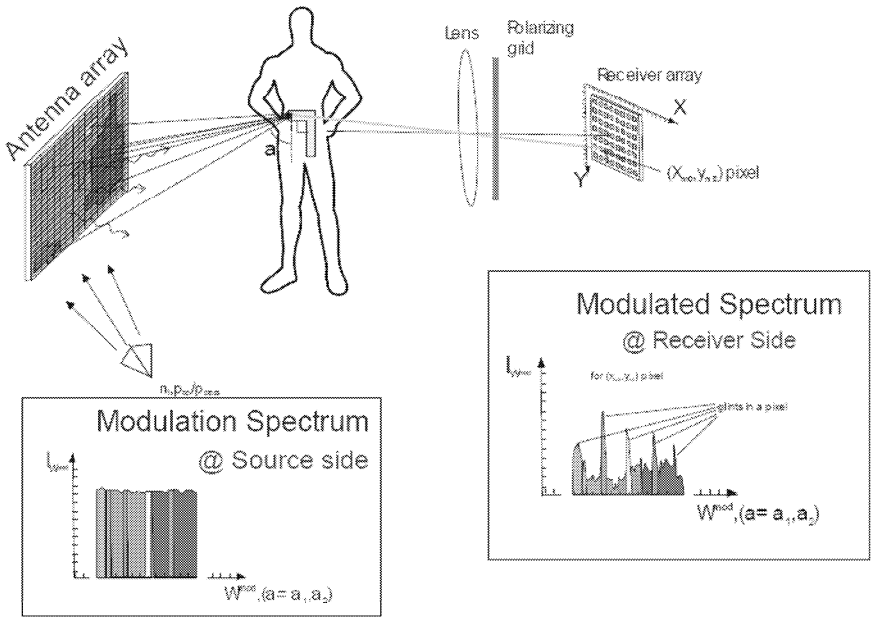


Fig. 1: Generic active millimeter wave imaging set-up for concealed weapon detection

## 2. MOTIVATION

This research originated within a project that has brought together people working in the fields of optical and THz imaging (VUB) with people from the EM-simulation field (UGent) and the millimeter wave electronics fields (KUL, Imec). The aim of the project is to establish a body of expertise in the field of active millimeter wave imaging within the region of Flanders. From discussing various system aspects it became clear that these systems fall into a gap between both types of engineering approaches and that each approach had to stretch their normal way of viewing these systems from a systems perspective. Hence, a very simple calculation method was proposed which could enable discussion on fundamental concepts and could serve as a rough optimization tool to develop active millimeter wave systems that are technologically feasible. Also, image enhancing techniques, such as despeckling, can be studied and modified to better suit the millimeter wave regime.

The conceptual gap can best be illustrated by scaling a typical millimeter wave imaging set-up to an optical equivalent (e.g. at 500 THz) and do the same towards lower frequencies (e.g. 1GHz). Indeed, a system such as depicted in Fig. 1 would typically scale to 500 THz as a 5 mm long optical system with lenses of 0.5 mm and objects of a few mm's being imaged onto a 2mm detector. Conversely, the lenses in a 1GHz system would be 50m in diameter with objects of 200m wide being imaged from a distance of 200m. Clearly, this shows how severe a problem the volume restriction is to achieve good imaging quality.

## 3. "1.5D" METHOD

Our proposed 1.5D model of the system (Fig. 2) is based on the following assumptions. Firstly, to simplify the geometry we assume that all component planes are parallel to each other and perpendicular to the propagation z-axis, i.e. the problem is reduced to a series of operations along a straight path from source to detector. In this way, the object is said to transmit power instead of reflecting it. Secondly, the problem is reduced to a 2D problem by assuming uniformity along the y-axis. Thirdly, the E-field is assumed perpendicular to the xz-plane, which further reduces the problem to the calculation of a single vector value. Fourthly, the field is assumed zero at large distances from the z-axis so that the number of points along the x-axis can be limited. Finally, reflections are neglected, so power flows only along the positive z-axis.

To further simplify the calculation, all system components are assumed infinitely thin and are characterized by their x-dependent complex transformation of the incident field. For the lenses, a geometrical optics thin-lens model is used to describe the lens, i.e. the effect of the lens on the incident field is a x-dependent complex number depending on the focal distance of the lens and the type of lens used and which can also incorporate propagation losses through the lenses. The method allows the use of any type of lens (spherical, parabolic, hyperbolic, flat…). In a similar way, simple descriptions of diffuser and object allow to quickly estimate speckle reduction for various types of objects and system set-up.

The horn antenna beam is modeled as a Gaussian beam of which the beam waist is estimated from a measured corrugated horn radiation pattern.

The calculation is carried out from one plane to the next using a quasi-optics ray tracing approach. The fields are calculated on a sufficient number of points on each component plane using the following formula:

$$E_2^j = \sum_{i=1}^{N} E_1^i . e^{\left(-j2\pi/\lambda d_{ij}\right)} / \sqrt{d_{ij}} \qquad (1)$$

where $E_2^j$ is the field on the j$^{th}$ point of the second component plane, $E_1^i$ is the field on the i$^{th}$ point of the first component plane, and $d_{ij}$ is the distance between the i$^{th}$ point on the first component plane and the j$^{th}$ point on the second component plane. The square root dependency on $d_{ij}$ is due to the y-independence assumption.

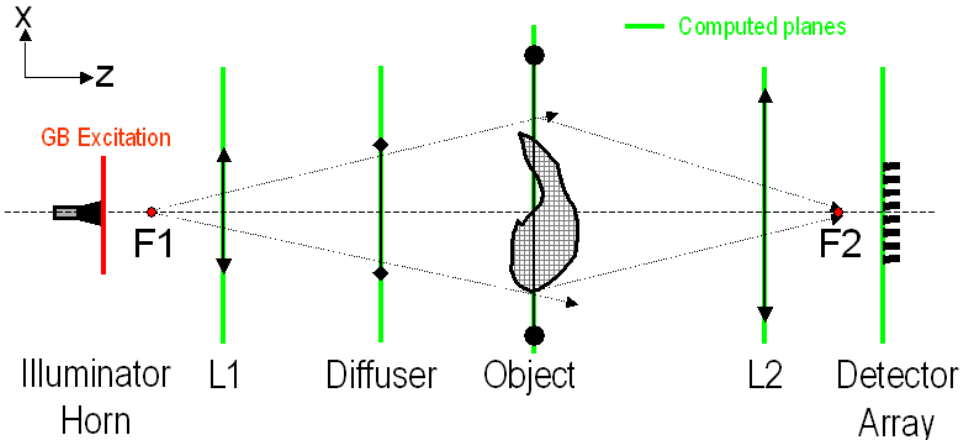


Fig. 2: System set-up used in the 1.5D model

The method, although limited in accuracy for practical systems still allows to do first order optimization for a complete system, before using more sophisticated methods for optimization. The limitation of the method is mostly due to the assumption that the E-field only has a component in the y-direction. The method, however, could be extended to a "2.5D" method by dropping this assumption and calculating all three field components on a square grid on the different planes.

## 4. FULL WAVE 2D METHOD

The proposed 1.5D method will be compared to a rigorous full-wave electromagnetic calculation [7], [8]. This two-dimensional scattering problem is treated using a Huygens source based boundary integral equation developed in [9]. Each object is divided into a number of segments, hence allowing for the inclusion of any polygonal objects. It is obvious that a realistic imaging system will constitute an amount of extremely large objects as compared to the wavelength, leading to a very large number of unknowns N.

The integral equation is solved numerically by application of the method of moments (MoM). Using iterative solvers, this gives rise to a computational complexity of $O(N^2)$. In order to accelerate the calculations and to keep the memory requirements within acceptable limits the MoM analysis is augmented with a High Frequency Multilevel Fast Multipole Technique (HF-MLFMA). This reduces the complexity of the computation and the required memory capacity to O(N). It allows the modeling of structures that are thousands of wavelengths in size.

In this particular case, the scenario consisted of lenses and an aperture with a total diameter of approximately 1000 wavelengths. The objects accounted for nearly 100,000 unknowns. Using the HF-MLFMA however, computation times are of the order of minutes while the memory requirements were below 1GByte. Using a devoted preconditioner, the number of iterations was only 221.

## 5. COMPARISON FOR REFERENCE SCENARIO

### 5.1. 1.5D method

The first system set-up which was calculated by the two methods is shown in Fig. 3. Illumination of the object is achieved using a horn/lens combination which focuses the Gaussian beam onto an object which is located 2m from the illuminator lens. The object is an aperture 25cm in diameter in an infinite resistive plane. An image of the object (taken to be the 25cm aperture together with 25cm of resistive material around it) is formed on a detector array consisting of 100 detector elements, spaced 5mm apart. This is done using a lens with diameter 50cm and radius of curvature of 1m. The relative E-field amplitudes and phases on the different component planes are shown in Figs. 4a and 4b. It is clear from the figure that the Gaussian character of the illuminating beam is maintained up to the object plane. Comparisons with Gaussian beam theory [5] have shown an agreement of better than 0.5%. Beyond the object plane the propagating beam is no longer Gaussian and diffraction is observed on the image formed on the detector array. We have verified the beam propagation at 100 GHz, using Gaussian beam theory, from the generator side (8 mm beamwaist) towards the object and from the detector side (5 mm beamwaist) towards the object, and comparisons of both methods show an agreement of better than 0.5% in magnitude and phase. As the main goal of this work is about the validation of the different simulation methods, we did not put large emphasis on the enhancement of the imaging characteristics of this system. These are evidently sub-optimal but they do agree with a realistic situation and are well suited for comparison.

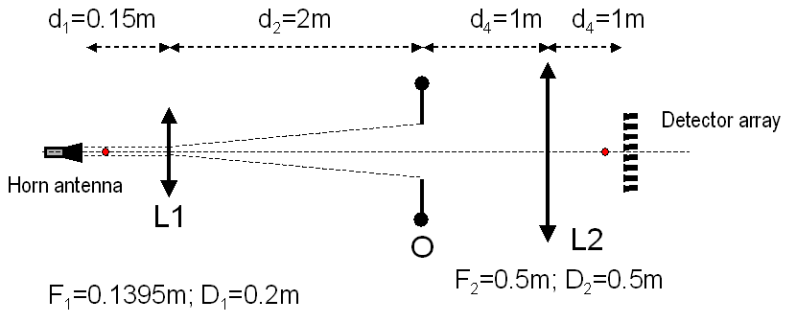


Fig. 3: System parameters for scenario1

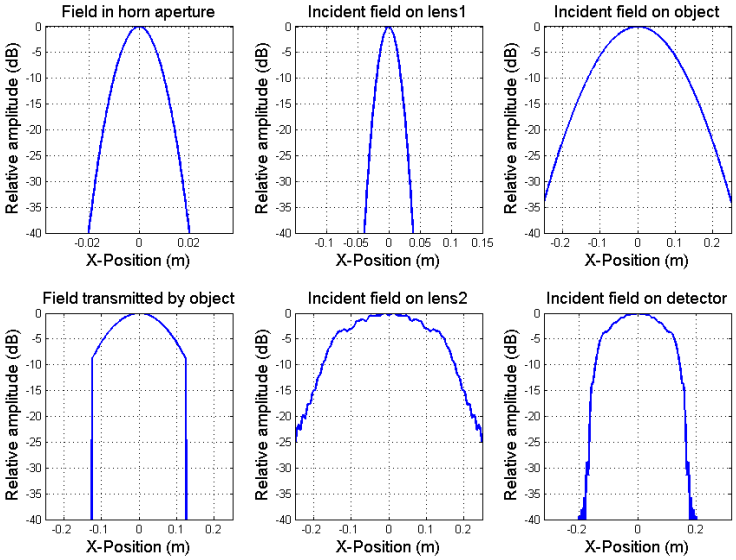


Fig. 4a: Amplitudes of incident fields calculated on different system planes

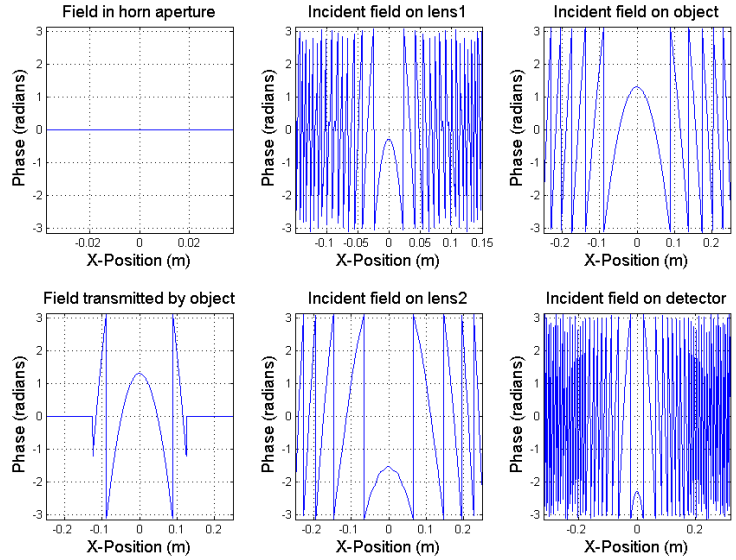


Fig. 4b: Phase of incident fields calculated on different system planes

### 5.2. 2D method

The same set-up as in the previous subsection was calculated using the full-wave 2D method. The calculated field distribution is shown in Fig. 5. From this figure it is clear that the Gaussian beam is focused in the same way as in the 1.5D method, but that reflections occur on the lens surfaces, which are neglected in the 1.5D method. This causes standing waves which are illustrated in Figs. 6 and 7, which show detailed images of the fields around the two lenses. A way to overcome this, which is also the way it is done for practical lenses, is to use an antireflective coating which will eliminate these reflections and reduce the formation of standing waves.

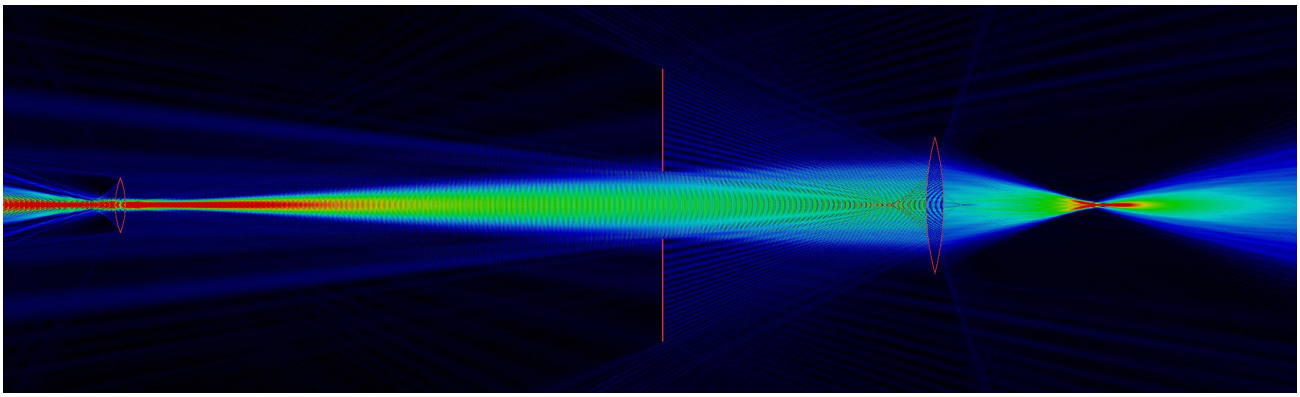

Fig. 5: 2D field distribution for reference scenario

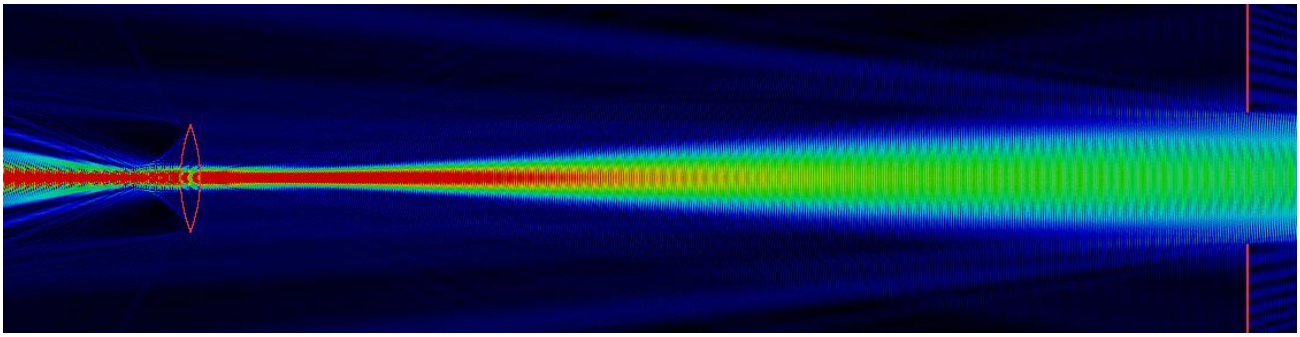

Fig. 6: 2D field distribution around illuminator lens

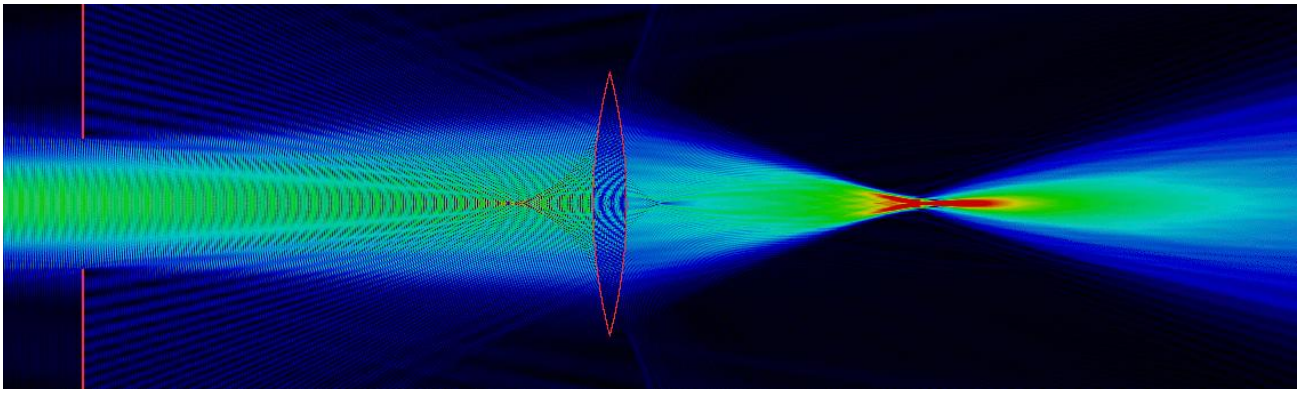

Fig. 7: 2D field distribution around detector lens

### 5.3. Comparison

The fields at the detector plane were compared for both methods and are shown in Fig. 8.

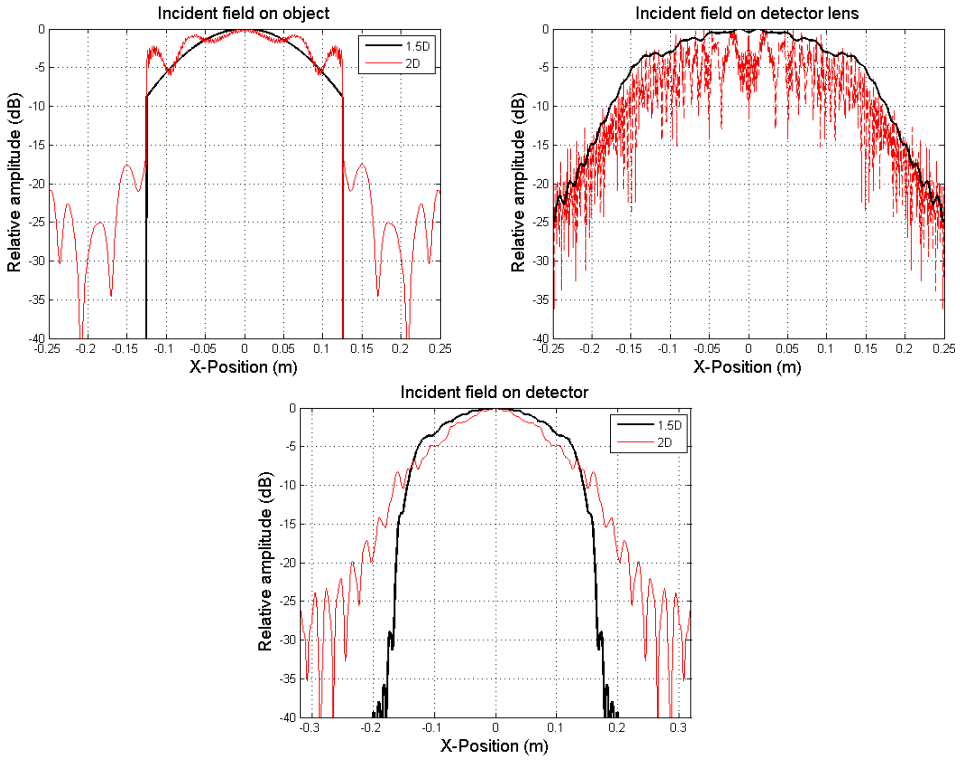


Fig. 8: Comparison of fields on object, detector lens and detector planes

### 5.4. Conclusions

In the previous sections the 1.5D and 2D methods were shown to give comparable results, although the agreement is limited because of lens reflections. Other sources of disagreement are also present, but difficult to gauge with the current set of results. More work is needed to take an anti-reflective coating into the 2D calculation and possibly, to include a single reflection in the 1.5D method.

In the subsequent sections some results are presented which were obtained with the 1.5D method, but these will have to be validated with comparable results obtained with the 2D method. This work is currently in progress and will be presented at the conference as it is available at that time.

## 6. EFFECT OF DETECTOR LENS ON IMAGE RESOLUTION

As we will show in section 8 on despeckling techniques, the success of the Hadamard diffuser techniques will in some part depend on the use of large lenses. In this section we will investigate the effect of lens diameter on detector resolution for a detector/sensor geometry which slightly differs from the reference scenario described in section 5. The detector lens has a focal distance of 1.2m, the distance between object and detector is 2m and the detector is an array of 100 detector elements spaced 7.5mm apart

To evaluate resolution, the PSF (Point Spread Function) was calculated which is the response of the imaging system to a point source as a radiating source. Figs. 9 and 10 show the evolution of this PSF as a function of detector lens diameter for a lens diameter varying between 0.1 and 2m; Table 1 gives the resolution dependency on f/D. The figures and table reveal a saturation of the attainable resolution because of a degradation of the PSF, which is due to the fact that the paraxial condition ($\sin\theta=\theta$) is no longer valid, causing severe aberrations. This illustrates the limitation that the Rayleigh criterion cannot be used below a certain value of f/D value of the lens, even for a lens modeled as infinitely thin. Also, this result indicates an optimum lens diameter to be used in an optimized imager. It also shows that the method could be used to synthesize lens shapes to increase imaging performance for small f/D lenses.

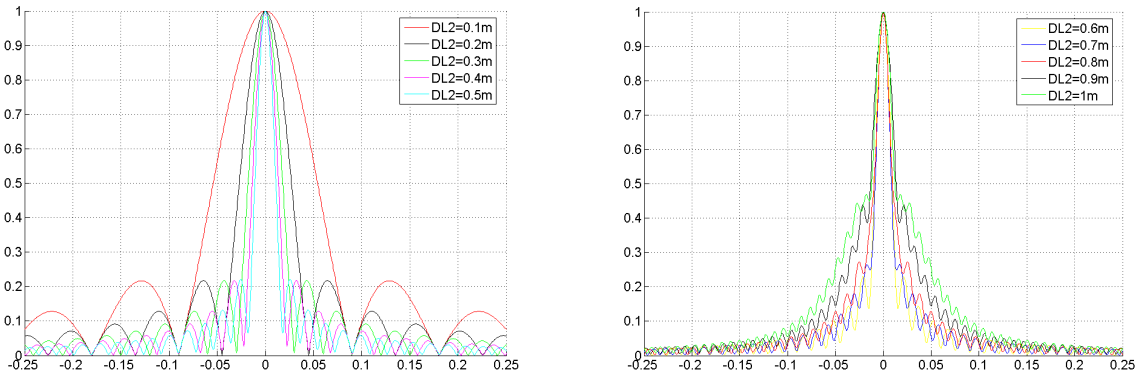


Fig. 9: PSF for lens diameters between 0.1m and 0.5m (left); PSF for lens diameters between 0.6m and 1m (right)

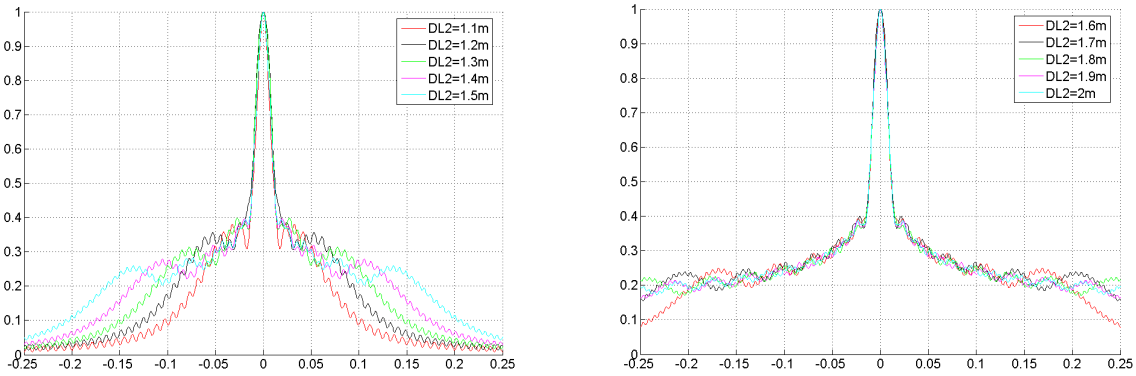


Fig. 10: PSF for lens diameters between 1.1m and 1.5m (left); PSF for lens diameters between 1.6m and 2m (right)

| f/D | 12 | 6 | 4 | 3 | 2.4 | 2 | 1.71 | 1.5 | 1.33 | 1.2 |
|---|---|---|---|---|---|---|---|---|---|---|
| Rayleigh criterion (mm) | 108 | 54 | 36 | 27 | 21.6 | 18 | 15.4 | 13.5 | 12 | 10.8 |
| Resolution spot (mm) | 80 | 40 | 26 | 20 | 16 | 13.6 | 12.2 | 12.6 | 19.8 | 17.4 |
| f/D | 1.09 | 1 | 0.92 | 0.85 | 0.8 | 0.75 | 0.7 | 0.66 | 0.63 | 0.6 |
| Rayleigh criterion (mm) | 9.81 | 9 | 8.3 | 7.7 | 7.2 | 6.75 | 6.35 | 6 | 5.68 | 5.4 |
| Resolution spot (mm) | 13.6 | 17.2 | 16.8 | 16.8 | 15 | 16 | 16.4 | 15.6 | 15. 8 | 16 |

Table 1: Effect of f/D on resolution

## 7. SPECKLE CHARACTERISATION

In order to evaluate speckle reduction techniques in section 8, we need a way of generating speckle, i.e. we need to model rough surfaces. This can be easily attained by modeling the phase of the object input/output relation as a square wave between 0° and 180° representing the response of the peaks and valleys of the surface, under the assumption that the valleys lie a quarter of a wavelength deeper than the peaks. The spatial period of the square wave was taken to be 5mm.

As a first simple model the surface is taken to have regularly spaced peaks and valleys. To see the effect of speckle in the case of the reference scenario, only half of the object surface is taken as rough, the other half is smooth. In Fig. 11

the image of a Gaussian beam on the detector array before and after applying the phase pattern is shown and clearly indicates the problem of speckle on the left half of the truncated Gaussian beam image.

An important question in this context is “What is the difference between surface roughness and image features?” since the first thing causes speckle, while the second thing is exactly what we are trying to see. When the number of phase changes per resolution cell in the above roughness model is large, then we would speak of “speckle”, while when this number of changes is small the imaging system would interpret it as an image feature. The value chosen here is neither small or large compared to the resolution cell size, so the effect illustrated by Fig. 11 is a combination of speckle and ringing. These considerations will need to be worked out in more detail, to understand what the image enhancement method should deal with exactly. A clear classification is needed of typical object roughnesses and what constitutes “speckle” and what is seen as an object feature, since this will have to be taken into account when designing despeckling techniques. These techniques will have to reduce speckle (high spatial frequency phase variations) while leaving the desired image features intact. The simple model could of course be extended to deal with random distributions of peaks and valleys to get a more realistic picture.

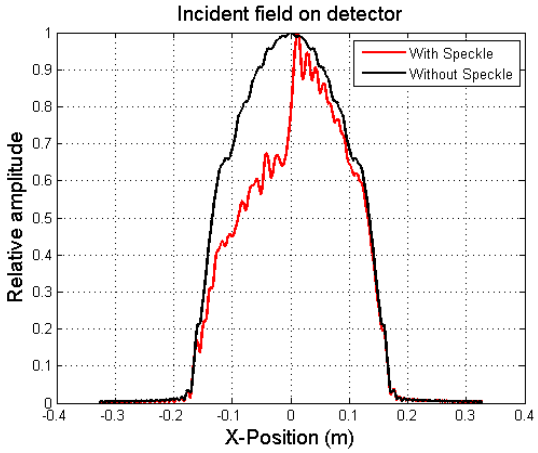


Fig. 11: Effect of applying speckle phase pattern

## 8. SPECKLE REDUCTION TECHNIQUES

### 8.1. Diffuser techniques

As depicted in Fig. 1 a known technique to reduce speckle is to use a diffuser to destroy the coherence of the illuminating beam. A set of orthogonal phase patterns is needed, such as described in [6], wherein the phase patterns are derived from the Hadamard matrix. Speckle reduction is based on averaging M independent (i.e. uncorrelated and non-interfering) speckle configurations within the spatial and temporal resolutions of the detector [6].

Applying this technique to the reference scenario results in the phase patterns being applied to each resolution cell size, i.e. on every 25cm/100=2.5mm of the object (truncated Gaussian beam). When e.g. 8 phase patterns are used, this means that the diffuser has to form phase patterns on the object with a spatial resolution of 2.5/8=0.4mm. We assume that the diffuser is able to achieve this task, and will model the image formation and averaging process to evaluate the performance of the despeckling approach. Figs. 12 and 13 show the image on the detector for the cases of 2 and 4 Hadamard phase settings, respectively, together with the averaged image.

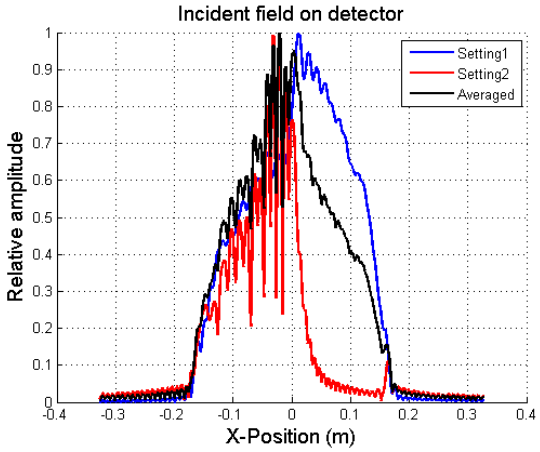


Fig. 12: Fields on detector plane for two Hadamard settings and the averaged field

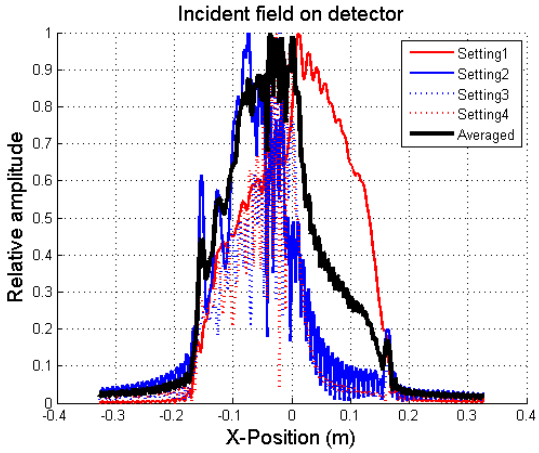


Fig. 13: Fields on detector plane for four Hadamard settings and the averaged field

The figures show that some speckle reduction can be achieved for the speckled left half of the truncated Gaussian beam, but that the patterns formed on the detector tend to have a distribution that is asymmetric, i.e. for negative values of x the amplitude is larger. The reason for this has to be sought in how the Hadamard phase patterns result in asymmetric power loss at the lens, i.e. the radiation is steered away from broadside. Because of this, the phase pattern is not correctly projected onto the detector array and the method premise is no longer valid. Two ways to avoid this are to use very large lenses which allow for more "beam steering" of the reflected field, or to choose a more favorable set of phase patterns which theoretically might not result in optimum speckle reduction, but also causes less "beam steering". These observations clearly indicate important system trade-offs to be made when using this technique.

The effect of detector radiation patterns and the resulting spatial averaging effect on the image was not yet considered, but will be in the near future and will be included in the conference presentation.

### 8.2. Multi-frequency techniques

Another technique which is being studied using the 1.5D method is the use of a broadband averaging technique to reduce speckle. The reference scenario with the "speckle" model of section 7 was studied for an averaging between 80GHz and 120GHz with steps of 1 GHz. Fig. 14 shows the resulting field distribution on the detector together with the averaged image, which indicates that in this case the averaged image is very close to the image at 100GHz, but with slightly attenuated oscillations for both sides of the truncated Gaussian beam. More work is clearly needed; this result was just added to show that these type of techniques can easily be evaluated by the method.

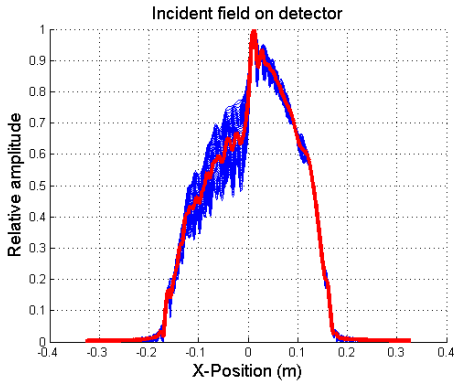


Fig. 14: Incident fields on detector array at frequencies between 80 GHz and 120 GHz (blue curves) together with the averaged field distribution (red curve)

## CONCLUSIONS

In this paper it was shown that a hybrid 1.5D/2D modeling approach for active millimeter wave imaging systems is a very useful tool in understanding image formation under coherent illumination. Using a reference scenario the 1.5D and 2D methods were compared and gave good agreement. The effect of antireflective coatings on the lenses was not yet taken into account by the 2D method, but will be implemented in the near future and will improve the agreement.

The 1.5D method was illustrated in a detector lens analysis and showed a lower limit for useful f/D values. From the sections on speckle a few important issues were raised such as the importance of phase settings and lens choice when using a Hadamard despeckling approach. The multifrequency technique was also briefly discussed.

## REFERENCES

1. Jurgen Detlefsen, Alexander Dallinger and Simon Schelkshorn, “Approaches to Millimeter-Wave Imaging of Humans”, European Radar Conference 2004, Amsterdam, pp. 279-282
2. David M. Sheen, Douglas L. McMakin, “Three-Dimensional Millimeter-Wave Imaging for Concealed Weapon Detection”, *IEEE Transactions on Microwave Theory and Techniques*, Vol. 49, No. 9, September 2001.
3. Leonid V. Volkov, Alexander I. Voronko, Natalie L. Volkova, Aram R. Karapetyan, “Active MMW Imaging Technique for Contraband Detection”, *33rd European Microwave conference*, Munich 2003, pp. 531-534.
4. P.F. Goldsmith, C.-T. Hsieh, G.R. Huguenin, J. Kapitzky and E.L. Moore, “Focal Plane Imaging Systems for Millimeter Wavelengths”, *IEEE Transactions on Microwave Theory and Techniques*, Vol. 41, No. 10, October 1993, pp. 1664-1675.
5. P.F. Goldsmith, Quasioptical systems”, Wiley-IEEE Press, 1997
6. J. I. Trisnadi, Hadamard speckle contrast reduction, Opt. Lett. 29(1), 11-13 (2004).
7. V. Rokhlin, "Rapid solution of integral equations of classical potential theory", J. Comp. Phys., 1985, vol.60
8. W. Chew, J. Jin, E. Michielssen, and J. Song, "Fast and Efficient Algorithms in Computational Electromagnetics" Artech House, 2001
9. F. Olyslager, D. De Zutter, and K. Blomme, “Rigourous analysis of the propagation characteristics of general lossless and lossy multiconductor transmission lines in multilayered media,” IEEE Trans. Microwave Theory and Techn., vol. MTT-41, no. 1, pp. 79-88, Jan. 1993

**Wednesday-Thursday 5-6 April 2006 • Proceedings of SPIE Vol. 6194**

# Millimeter-Wave and Terahertz Photonics

*Conference Chairs:* **Dieter Jäger**, Univ. Duisburg-Essen, OpTech-Net e.V. (Germany); **Andreas Stöhr**, Univ. Duisburg-Essen (Germany)

*Program Committee:* **Béatrice Cabon**, École Nationale Supérieure d'Electronique et de Radioélectricité de Grenoble (France); **Stephane Formont**, THALES Airborne Systems (France); **M. Hofman**, Ruhr-Univ. Bochum (Germany); **Alwyn J. Seeds**, Univ. College London (United Kingdom)

***Conference 6194 contains a paper funded by and/or related to current EU research projects contained in Framework VI.***

*Paper Numbers:* 1, 10.

## Wednesday 5 April

### SESSION 1

**Orangerie . . . . . Wed. 13.30 to 15.10**

**RF Photonics**

*Chair:* **John E. Mitchell**, Univ. College London (United Kingdom)

13.30: **Joint European research projects in millimetre-wave and THz photonics, ISIS and IPHOBAC,** B. Cabon, École Nationale Supérieure d'Electronique et de Radioélectricité de Grenoble (France); A. Stöhr, Univ. Duisburg-Essen (Germany) . . . . . [6194-01]

13.50: **Demonstration of overlay UMTS signal transmission on a gigabit passive optical network,** H. Le Bras, D. Schumacher, M. Moignard, France Télécom (France) . . . . . [6194-02]

14.10: **Microwave photonic cross-connect repeater for telecommunication satellites,** B. Benazet, Alcatel Alenia Space (France); M. Sotom, Alcatel Alenia space (France); M. Maignan, Alcatel Alenia Space (France); J. M. Perdigues Armengol, European Space Research and Technology Ctr. (Netherlands) . . . . . [6194-03]

14.30: **Data transmission using a spectrum sliced radio over fibre link,** J. E. Mitchell, Univ. College London (United Kingdom) . . [6194-04]

14.50: **Optical carrier proccessor of microwave/millimeter-wave photonic signals by using a fiber Bragg grating in transmission,** M. J. Erro, R. Hernández, A. Loayssa, Univ. Pública de Navarra (Spain); J. Mora, Univ. Politècnica de València (Spain); D. Benito, Univ. Pública de Navarra (Spain) . . . . . [6194-05]

## Thursday 6 April

### SESSION 2

**Orangerie . . . . . Thurs. 10.30 to 12.40**

**Mm-wave and THz: Spectroscopy and Imaging**

*Chair:* **Johan H. Stiens**, Vrije Univ. Brussel (Belgium)

10.30: **Applications of semiconductor terahertz lasers in biomolecular spectroscopy and imaging *(Invited Paper)*,** E. Bruendermann, M. Havenith, Ruhr-Univ. Bochum (Germany) . [6194-06]

11.00: **Investigation of water and soot contamination in petroleum products via terahertz transmission spectroscopy,** S. Gorenflo, U. Tauer, I. Hinkov, A. Lambrecht, Fraunhofer-Institut für Physikalische Messtechnik (Germany); H. Helm, Albert-Ludwigs-Univ. Freiburg (Germany) . . . . . [6194-07]

11.20: **Terahertz time-domain spectroscopy and spectrochronography of amino acids and polypeptides,** A. P. Shkurinov, A. Chikishev, S. Shkelnyuk, M. Nazarov, D. Sapozhnikov, I. Smirnovs, M.V. Lomonosov Moscow State Univ. (Russia); O. Okhotnikov, Tampereen Teknillinen Yliopisto (Finland) . . . . . [6194-08]

11.40: **Characterization of speckle/despeckling in active millimeter wave imaging systems using a first-order 1.5D model,** I. Ocket, B. Nauwelaers, Katholieke Univ. Leuven (Belgium); L. Meert, F. Olyslager, Ghent Univ. (Belgium); G. Koers, J. H. Stiens, R. A. Vounckx, I. Jager, Vrije Univ. Brussel (Belgium) . . . . . [6194-09]

12.00: **Semi-confocal imaging with a THz gas laser,** M. A. Salhi, M. Koch, Technische Univ. Braunschweig (Germany) . . . . . [6194-10]

12.20: **Speckle reduction in THz imaging systems with multiple phase patterns,** I. Jager, J. H. Stiens, R. A. Vounckx, G. Koers, G. Poesen, Vrije Univ. Brussel (Belgium) . . . . . [6194-11]

Lunch Break . . . . . 12.40 to 13.50

### SESSION 3

**Orangerie . . . . . Thurs. 13.50 to 15.40**

**Mm-wave and THz: Photomixer**

*Chair:* **Dieter Jäger**, Univ. Duisburg-Essen (Germany)

13.50: **High-responsibility, broadband waveguide uni-travelling carrier photodiode *(Invited Paper)*,** C. C. Renaud, Univ. College London (United Kingdom); M. Robertson, D. Rogers, R. Firth, P. J. Cannard, R. Moore, Ctr. for Integrated Photonics Ltd. (United Kingdom); A. J. Seeds, Univ. College London (United Kingdom) . . . . . [6194-14]

14.20: **THz Photomixers: an overview,** A. Stöhr, D. Jäger, Univ. Duisburg-Essen (Germany) . . . . . [6194-15]

14.40: **Total field-emission properties of terahertz radiations by plasmon-resonant photomixer,** Y. M. Meziani, Tohoku Univ. (Japan) . . . . . [6194-12]

15.00: **Highly collimated and directed (cw) THz emission by photomixing in semiconductor device arrays,** S. Malzer, S. Preu, G. H. Döhler, Z. Lu, J. Zhang, L. Wang, Friedrich-Alexander-Univ. Erlangen-Nürnberg (Germany) . . . . . [6194-13]

15.20: **A numerical study of photoconductive dipole antennas: the real emission frequency and an improved antenna design,** K. Ezdi, M. N. Islam, A. N. R. Yerrappareddy, C. Jördens, A. Enders, M. Koch, Technische Univ. Braunschweig (Germany) . . . . . [6194-16]

Coffee Break . . . . . 15.40 to 16.00

### SESSION 4

**Orangerie . . . . . Thurs. 16.00 to 17.40**

**Mm-wave and THz: Optical Sources, Detectors, and Filters**

*Chair:* **Erik Bründermann**, Ruhr-Univ. Bochum (Germany)

16.00: **Room-temperature terahertz generation with semiconductor lasers,** C. Brenner, T. N. Le, S. Hoffmann, M. R. Hofmann, Ruhr-Univ. Bochum (Germany) . . . . . [6194-17]

16.20: **InN as THz emitter excited at 1060 nm,** B. Pradarutti, C. Brückner, S. Riehemann, G. Notni, A. Tünnermann, Fraunhofer-Institut für Angewandte Optik und Feinmechanik (Germany); G. Matthäus, S. Nolte, Friedrich-Schiller-Univ. Jena (Germany); V. Cimalla, O. Ambacher, Technische Univ. Ilmenau (Germany) . . . . . [6194-18]

16.40: **Two-mode operation of four-section semiconductor laser for THz generation by photomixing,** A. Akwoue Ondo, J. Torres, C. Palermo, L. Chusseau, Univ. Montpellier II (France); J. Jacquet, Supélec (France); M. Thual, École Nationale Supérieure des Sciences Appliquées et de Technologie (France) . . . . . [6194-19]

17.00: **Femtosecond electron gun for diffraction experiments,** E. E. Fill, A. A. Apolonskiy, F. Krausz, Max-Planck-Institut für Quantenoptik (Germany) . . . . . [6194-26]

17.20: **Improved dielectric mirrors for the THz frequency range,** F. Rutz, N. Krumbholz, Technische Univ. Braunschweig (Germany); L. Micele, G. De Portu, Consiglio Nazionale delle Ricerche (Italy); D. M. Mittleman, Rice Univ. (USA); M. Koch, Technische Univ. Braunschweig (Germany) . . . . . [6194-20]

Technical Programme

# Photonics EUROPE

An SPIE Europe Event

*3–7 April 2006*
*Palais de la Musique et des Congrès • Strasbourg, France*

The only event that bridges research and commerce.

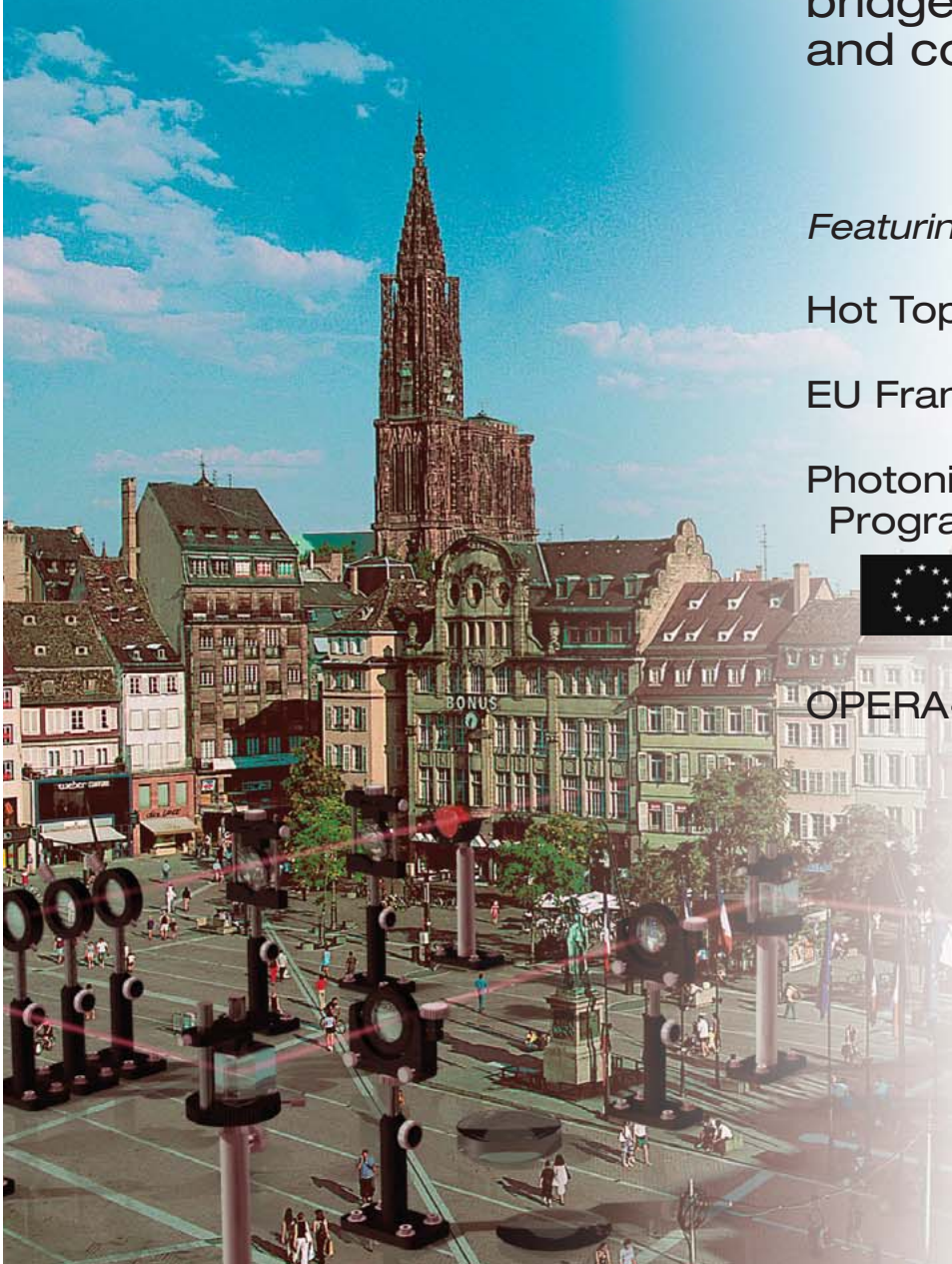

*Featuring:*

Hot Topics

EU Framework News

Photonics Industry Programme

*Under the patronage of the EC*

OPERA-2015 Workshop

SPIE *Europe*